THE DOUBLE FIXED CHARGE MEMBRANE

Low Frequency Dielectric Dispersion

H. G. L. COSTER

From the School of Physics, University of New South Wales, Sydney, Australia

ABSTRACT An analysis is made of the AC characteristics of a membrane consisting of two fixed charge regions of opposite sign, in contact. It is shown that the equivalent parallel capacitance and conductance of such a membrane undergo a strong dispersion at low frequencies. The dielectric dispersion is a result of polarization effects in the diffusion of coions in each of the two fixed charge lattices. This, at low frequencies, gives rise to a very large diffusion capacitance. The form of the dispersion characteristics is very similar to those observed for synthetic-fused anion-cation membranes and various cellular membranes.

INTRODUCTION

In an elegant, now classical, series of experiments it was established that the observed total impedance loci of various biological materials could be accounted for if the cell membrane contained a frequency-dependent impedance element of constant phase angle (Cole, 1928, 1932, 1965, 1968; Cole and Curtis, 1938, 1939). The presence of such an impedance element in the cell membrane was inferred from the circular arc form of the "Cole-Cole" plots of the real vs. the imaginary parts of the total impedance. The Cole-Cole plots further indicated that changes that take place in the membrane impedance, for instance in the presence of DC currents, largely reflect changes in the leakage resistance of the membrane. The capacitive element, however, itself was inferred to be also "lossy;" though having a phase angle substantially independent of frequency.

At very low frequencies, below 1 kHz in squid axons, an additional dielectric dispersion phenomenon is observed (e.g., see Schwann, 1954, 1957; Schwann and Carstensen, 1957; Cole, 1970). In this very low frequency region the membrane capacitance increases with decreasing frequency.

Recent experiments with the giant cells of *Chara corallina* (previously *C. australis*),[1] using internal longitudinal platinum/irridium electrodes in a four-terminal configuration, have shown that for the membranes of these cells the low frequency

[1] Coster, H. G. L., and J. Smith. Manuscript in preparation.

dispersion commences at 1 Hz or less. Plots of the real vs. the imaginary part of the complex impedance of the membrane itself yielded approximately semicircular loci, which, extrapolated to infinite frequency, pass through the origin. At higher frequencies (>200 Hz) the total membrane capacitance, but not the conductance, becomes almost frequency independent.

The electric current through biological membranes, when an AC or DC bias is applied, arises from the diffusion of ions down the gradients in their electrochemical potentials established by the applied bias. The diffusion process is associated with polarization effects which give rise to a relaxation phenomenon (see Cole 1965; Offner, 1969).

The present communication is concerned with the diffusion of ions through a double fixed charge membrane (FCM) under the influence of an AC signal. It will be shown that the double FCM model can account for the low frequency impedance dispersion of the cell membrane and the results of Schwartz and Case (1964) for synthetic-fused cation-anion membranes. This is particularly of interest since this theoretical model also successfully accounts for a variety of other electrical and electrochemical effects observed in cellular membranes (Coster, 1965, 1969, 1972; Coster and Hope, 1968).

THE DOUBLE FCM MODEL

The system to be considered here has been described previously (e.g., Coster, 1965). It consists of a region of fixed positive charges (concentration N^+) in contact with a region of fixed negative charges (concentration N^-). The fixed charges are imbedded in an inert matrix which is permeated by an ionic solution. For the analysis the nature of the fixed charges need not be specified, although in the cell membrane they could arise from the dissociation of free amino or carboyxl groups on membrane proteins (Coster, 1969).

The junction of the fixed positive charge lattice with the fixed negative charge lattice gives rise to a transition region (depletion layer) in which the mobile ions have a very low concentration and the space charge density is consequently very high (see Mauro, 1962; Coster, 1965). When a bias is applied to the system, changes in the ion profiles lead to a storage of charge in the membrane and the system therefore displays the property of capacitance.

IONIC CURRENTS IN THE DOUBLE FCM

The DC electrical characteristics of the double FCM have been discussed in detail in our previous communications. The method of analysis which will be used in the present work is the simplified analytical method used earlier (Coster, 1965). Computer solutions of the field equations (Coster et al., 1969) for the double FCM have verified that, at least for a 100 Å membrane, the former analysis[2] is substantially

[2] It is assumed in the present analysis that $N^+ \gg \gamma_P P_0$ and $N^- \gg \gamma_N N_i$, where P_0 is the cation concentration in the external solution, N_i is the anion concentration in the "internal" solution on the

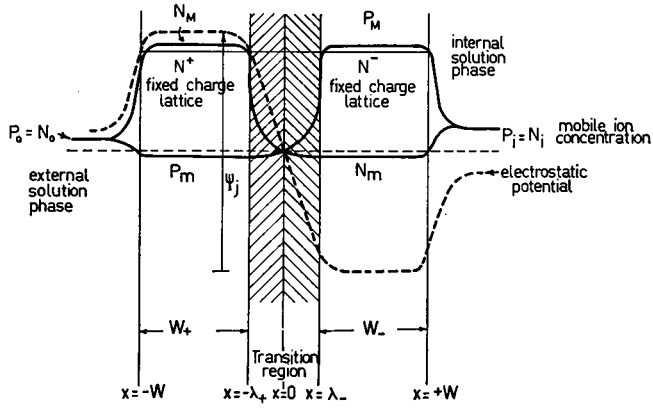

FIGURE 1 Qualitative profiles for the electrostatic potential (dashed curve) and the mobile ion concentration, for the double FCM in which the left half of the membrane contains fixed positive charges and the right half contains fixed negative charges. The region near the abrupt junction of the two lattices (transition region or depletion layer) is almost completely depleted of mobile ions and subsequently the space charge density there is high.

correct for a wide range of applied potentials. An outline of some of the basic features required for the present analysis is given below.

At zero applied bias the minority (coions) in one lattice, for instance the N^+ lattice, are in equilibrium with the majority, counterions in the opposite (N^-) lattice. (see Fig. 1). The concentration of the ions are related by

$$P_m = P_M \exp - q\psi_j/kT, \tag{1}$$

where ψ_j is the junction potential between the N^+ and N^- lattices, P_m is the coion minority concentration of positive ions in the N^+ lattice, and P_M is the counterion majority concentration of positive ions in the N^- lattice.

The transition layer is almost completely depleted of mobile ions and therefore has a relatively high electrical resistance compared with other regions in the membrane. A bias applied to the membrane therefore appears almost completely across the depletion layer.

The changes in the ion profiles resulting from changes in the electrostatic potential when a bias is applied can again be determined with the aid of the Boltzmann equation (see Coster, 1965; Coster et al., 1969). The changes in ion concentrations are confined to the minority coions in each lattice, the values at the depletion layer boundary being given by (see also Fig. 3, Coster, 1965),

$$P_j = P_M \exp - q(\psi_j - V)/kT = P_m \exp qV/kT. \tag{2}$$

other side of the membrane, γ_P, γ_N are the solution-membrane partition coefficients for the ions. The condition, above, which takes into account the ion partition effects (Coster, 1973), replaces the more stringent condition $N^+ \gg P_0$, $N^- \gg N_i$ required for the validity of the analysis previously given.

A similar expression holds for the coions (anions) in the N^- lattice.

A change in the counterion concentration in a similar ratio would lead to very high values of space charge. This, from energetic considerations, therefore, does not occur.

Under bias the coion concentrations P_j and N_j, at the depletion layer boundary, are not in equilibrium with the coions in the remainder of the lattice outside the depletion layer. The DC current in the membrane arises from the diffusion of the coions down their concentration gradients. In the steady state this concentration varies linearly between the value P_m at the solution-membrane boundary to P_j at the depletion layer boundary. The current density is then given by,

$$I_P = qD_P \frac{dP}{dx} = qD_P \frac{P_j - P_m}{W - \lambda_+},$$

$$= q \frac{D_P P_m}{W - \lambda_+} (\exp qV/kT - 1). \qquad (3)$$

Here W is the total width of the N^+ lattice, D_P is the diffusion constant for cations in this lattice, and λ_+ is the width of the depletion layer in the N^+ lattice.[3] A similar expression holds for the anions. The bracketed term in the expression 3 gives rise to the rectification properties of the system. It should be noted that the width of the depletion layer λ_+ increases with increasing reverse (hyperpolarizing) bias (i.e., negative).[4]

THE LOW FREQUENCY AC CHARACTERISTICS

In the following analysis it will be assumed, for simplicity, that the applied AC potential is small. In calculating the diffusion of coions therefore the width of the depletion layer can be taken as constant. Nevertheless the small modulation of the depletion layer width, of course, still gives rise in the normal way to the junction capacitance discussed by Mauro (1962).

With an AC signal applied to the membrane, the concentration of coions in each lattice will again be modulated as described above. The concentrations, however, will now be both space and time dependent (see Fig. 2).

The following considerations apply to the coions (cations) in the N^+ lattice. An entirely analogous situation exists for the anions in the N^- lattice. It will be assumed that the principle of superposition remains valid and the space and time dependence of the ion concentrations can be separated by writing:

$$P = P(x, t) = f(x) \cdot g(t) + h(x), \qquad (4)$$

where h is the DC component.

---

[3] Here for simplicity of notation λ_+ and W_+ replace λ_{N^+} and W_{N^+} as used in our previous communications.

[4] This eventually leads to the punch-through effect (Coster, 1965, 1969), in which the slope conductance increases very rapidly with hyperpolarization.

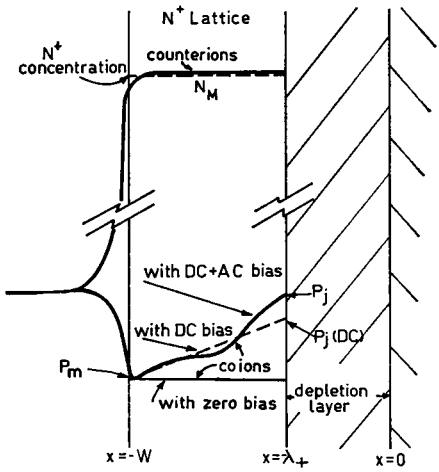

FIGURE 2 Qualitative profiles for the counterions (anions, N_M) and the coions (cations, P_m), in the region outside the depletion layer in the N^+ lattice, when an AC signal is superimposed on a DC potential applied to the membrane. The dashed line indicates the corresponding coion profile for the DC bias only. The coion profile at zero bias is also indicated. P_j is the coion concentration at the depletion layer boundary at $x = -\lambda_+$. Note that the profiles of ion concentration *outside* the depletion layer are modulated by the applied DC bias and/or AC signal which itself appears almost entirely across the depletion layer.

The method of solution of this equation is formally similar to that for the diffusion polarization given by Cole (see Cole, 1968). The electric field in the fixed charge lattices outside the depletion layer is negligible, hence, unlike the considerations of Offner (1969), the chemical or osmotic diffusion force, in complete analogy with Cole's work, dominates the diffusion.

As in our previous considerations of the double FCM model it will again be assumed that the ionic solution permeating the membrane is a strong electrolyte; that is, it is fully dissociated. The coions therefore obey the following continuity equation.

$$\frac{\partial P}{\partial t} - D_P \frac{\partial^2 P}{\partial x^2} = 0. \tag{5}$$

Combining Eqs. 4 and 5 and making use of the fact that the gradient of the DC component is constant then yields

$$\frac{1}{g(t)} \frac{\partial}{\partial t} g(t) = K,$$

and

$$\frac{D_P}{f(x)} \frac{\partial^2}{\partial x^2} f(x) = K, \tag{6}$$

where K is a constant.

The solution of these equations is subject to the following two boundary conditions. (*a*) At the membrane-solution boundary, $x = -W$, the coion concentration is time independent and equal to P_m. (*b*) At the depletion layer boundary, $x = -\lambda_+$, the concentration of coions is modulated by the applied bias and can, as in the case of a DC bias, be determined with the aid of the Boltzmann equation.

The applied bias V now contains an AC component, that is,

$$V = V(\mathrm{DC}) + \tilde{V} \exp j\omega t. \tag{7}$$

If the amplitude $\tilde{V}$ of the AC component is small the coion concentration at the depletion layer boundary is, using Eqs. 2 and 7, given by

$$P_j = P_j(t) = P_m \exp \frac{qV(\mathrm{DC})}{kT} \left[1 + \frac{q\tilde{V}}{kT} \exp j\omega t\right]. \tag{8}$$

The changes in coion concentrations will now be propagated through the N^+ lattice as an attenuated wave.

With the two boundary conditions above, the Eqs. 6 yield the following expression for the coion concentration (see Appendix).

$$P(x, t) = \tilde{P}_j \left\{ \frac{\exp\left[(W + x)\sqrt{j\omega/D_P}\right] - \exp - \left[(W + x)\sqrt{j\omega/D_P}\right]}{\exp + \sqrt{j\omega W_+^2/D_P} - \exp - \sqrt{j\omega W_+^2/D_P}} \right\} \cdot \exp j\omega t + h(x), \tag{9}$$

where h is the DC component; $\tilde{P}_j$ is the amplitude of the AC variation of P at the depletion layer boundary and is given by

$$\tilde{P}_j = P_j(\mathrm{DC}) \frac{q\tilde{V}}{kT} = \left(P_m \exp \frac{qV(\mathrm{DC})}{kT}\right) \frac{q\tilde{V}}{kT}; \tag{10}$$

and $W_+ = W - \lambda_+$ is the width of the N^+ lattice outside the depletion layer.

The current density is obtained in the same way as before from the slope of the coion concentration at $x = -\lambda_+$. Thus the AC component of the current density is given by,

$$\tilde{i}_P = -q D_P \left.\frac{\partial \tilde{P}}{\partial x}\right|_{x=-\lambda_+},$$

$$= q D_P \tilde{P}_j \sqrt{\frac{j\omega}{D_P}} \left[\frac{1 + \exp 2\sqrt{\frac{j\omega}{D_P}} W_+^2}{1 + \exp 2\sqrt{\frac{j\omega}{D_P}} W_+^2}\right] \exp j\omega t. \tag{11}$$

Substituting for $\tilde{P}_j$ from Eq. 10 and using the expression 3 for the DC current

density, the expression for the AC current density carried by cations takes the simple form:

$$\tilde{i}_P = (I_P + I_{PS}) \frac{q\tilde{V}}{kT} \sqrt{\frac{j\omega}{D_P} W_+^2} \coth \sqrt{\frac{j\omega}{D_P} W_+^2} \cdot \exp j\omega t. \qquad (12)$$

Here I_P is the DC current density carried by cations and I_{PS} is the corresponding reverse saturation current (i.e., when $V \ll 0$) which would be present if the depletion layer width always remained small compared with the total width of the N^+ lattice. Thus from Eq. 3

$$I_{PS} = \frac{q D_P P_m}{W_+}. \qquad (13)$$

Analogous expressions hold for the anions.

LOW FREQUENCY IMPEDANCE

The applied potential which gives rise to the current given by Eq. 12 appears across the depletion layer. Thus the contribution to the impedance defined by $Z(P) = \tilde{V}/\tilde{i}_P$, due to the diffusion of cations, is given by

$$Z(P) = \frac{\tilde{V}}{\tilde{i}_P} = \frac{kT \tanh \sqrt{\frac{j\omega}{D_P} W_+^2}}{q(I_P + I_{PS}) \sqrt{\frac{j\omega}{D_P} W_+^2}}. \qquad (14)$$

A similar expression holds for the anions and since the total AC current is the sum of $\tilde{i}_P$ and $\tilde{i}_N$ the total impedance is

$$Z = \left[\frac{1}{Z(P)} + \frac{1}{Z(N)}\right]^{-1}, \qquad (15)$$

Each of the terms $1/Z(P)$ and $1/Z(N)$ may of course contain contributions from more than one ion species. For instance the admittance $1/Z(P)$ of the N^+ region in the biological membrane would contain contributions from the (minority) sodium and potassium ions.

Inspection of Eq. 14 reveals[5] that the impedance due to diffusion limitation of the mobile ions contains frequency-dependent resistive and reactive components. When the two fixed charge lattices have different widths and/or the diffusion constants D_P and D_N are different, the frequency dependence of Z is further complicated because of differences in the frequency dependence of $Z(P)$ and $Z(N)$.

[5] The complex nature of this impedance can be more readily seen by noting that $\tanh \sqrt{jX^2} = [\tanh (X/\sqrt{2}) + j \tan (X/\sqrt{2})]/[1 + \tanh (X/\sqrt{2}) \times j \tan (X/\sqrt{2})]$

Apart from the impedance given by Eq. 15 the depletion layer also has a capacitance due to the storage of charge, as discussed by Mauro (1962). This capacitance, per unit area, which appears as a reactive element in parallel with the impedance given by Eq. 15, is given by

$$C = \frac{\epsilon_0 \epsilon_R}{2\lambda} , \qquad (16)$$

where ϵ_R is the relative electric permittivity (dielectric constant)and ϵ_0 is the permittivity of free space.

DIELECTRIC DISPERSION: NUMERICAL RESULTS

The nature of the dispersion indicated by Eqs. 14, 15, and 16 is most readily seen by considering numerical values of the impedance and admittance at various frequencies for appropriate numerical values of the various membrane parameters. As the results are intended merely as an illustration of the type of dispersion to be expected, no attempt was made to pinpoint the exact values of the parameters. The values chosen, however, which are listed in Table I are: (*a*) physiologically reasonable, and (*b*) are required to fit typical DC electrical characteristics for the membranes of cells of *C. corallina* (see also footnote on Table I and Discussion).

The results presented are therefore aimed at accounting for the dispersion charac-

TABLE I

VALUES OF THE FCM PARAMETERS USED IN THE NUMERICAL CALCULATIONS

(The values listed are appropriate for cells of *C. corallina*)

Parameter	Value	Comment
$\frac{kT}{q(I_P + I_{PS})}$	80 kΩ cm²	Gives a typical total membrane DC resistance* of 40 kΩ cm² at zero current (i.e., when $I_P = I_N = 0$)
W	50 Å	Total membrane thickness $2 \times W = 100$ Å
$W_+ (= W_-)$	35 Å	i.e., for a depletion layer of width $\lambda_+ = \lambda_- = 15$ Å in each lattice. (see Coster et al., 1969)
$W_\pm^2/D$	0.1, 0.2, 0.4 S (see also comment below)	This range is in accord with the DC resistance* when $N^+ = N^- \sim 0.1\ N$
C_j [depletion layer capacitance]	1 μF/cm²	In accord both with experimental values at frequencies $\gtrsim$200 Hz and theory, see Coster et al., 1969.

* The diffusion constants used in the calculations are averaged over the whole membrane. If localized regions exist (e.g., pores) the diffusion constants in these regions will be much larger and hence the diffusion capacitances in these regions much smaller. As long as the ion profiles are established in the remainder of the membrane, however, the total frequency-dependent diffusion capacitance will remain substantially unaltered. The frequency dependence of the total conductance, however, would be substantially modified, see Discussion.

teristics of these particular cells. The theory could, however, be equally well applied to other systems.

Dispersion Characteristics

Cole-Cole plots of the *membrane* impedance, including the junction capacitance, for values of $W_{\pm}^2/D$ = 0.4, 0.2, and 0.1 S. are shown in Fig. 3. It is evident that the

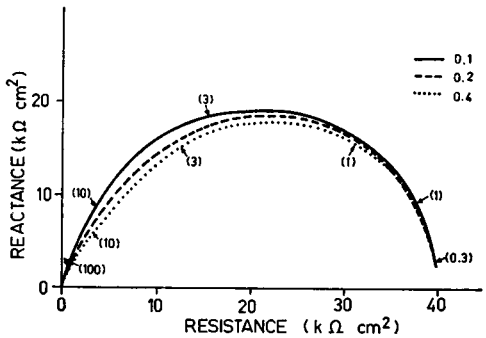

FIGURE 3 A plot of the equivalent series reactance ($-jX$) vs. the resistance (R) of the complex impedance of the double FCM for values of $W_{\pm}^2/D$ = 0.1, 0.2, and 0.4 S (D is the diffusion constant, $W_{\pm}$ is the width of the regions outside the depletion layer in each lattice). The number in brackets indicate frequencies in hertz. The total DC resistance of the membrane was set at 40 kΩ cm². The values of the other parameters injected into the numerical calculations are listed in Table I.

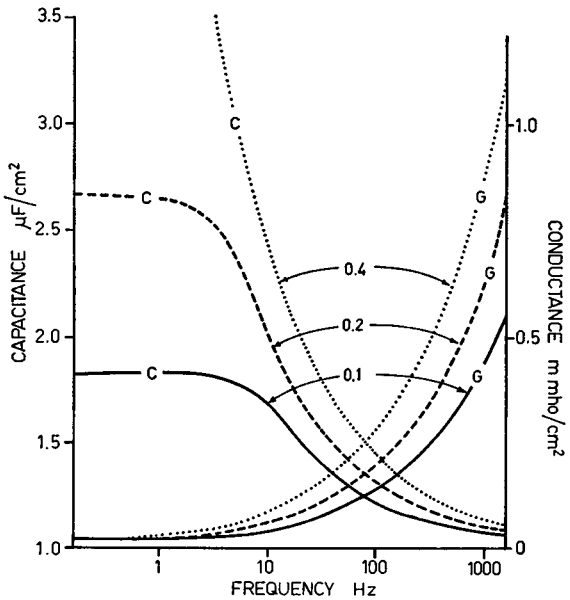

FIGURE 4 The equivalent parallel capacitance and conductance of the double FCM as a function of frequency for membranes with $W_{\pm}^2/D$ = 0.1, 0.2, and 0.4 S. Note that at high frequencies the capacitance approaches a value of 1 μF/cm² which is the value of the depletion layer capacitance.

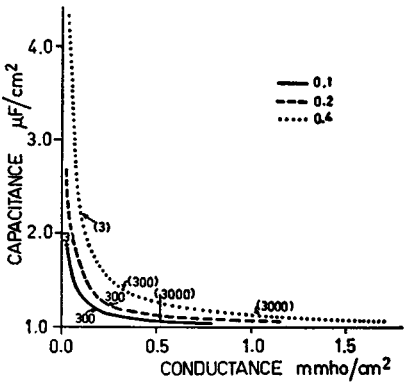

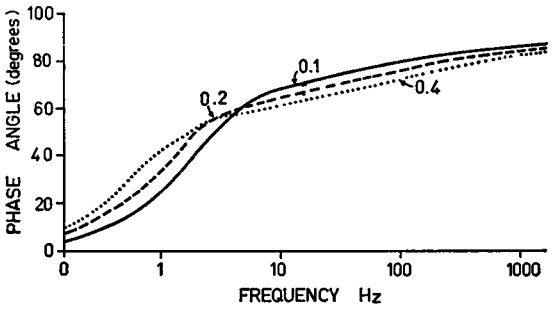

FIGURE 5

FIGURE 6

FIGURE 5 The parallel capacitance as a function of the conductance for membranes with $W_{\pm}^2/D = 0.1$, 0.2, and 0.4 S. The numbers in brackets indicate frequency in hertz.

FIGURE 6 The phase angle of the complex impedance as a function of frequency for double FCM's with $W_{\pm}^2/D = 0.1$, 0.2, and 0.4 S.

impedance loci are approximately semicircular. Note, however, the low frequencies involved (frequencies shown in brackets).

An important feature of the results is that the impedance variations are not restricted to the resistive part but also involve the reactive component. This is probably most easily seen by reference to Fig. 4 which shows the equivalent parallel conductance and capacitance of the membrane as a function of frequency, again for $W_{\pm}^2/D = 0.4$, 0.2, and 0.1 S.

It is immediately evident that both C and G show a very strong dispersion. The capacitance eventually, asymptotically, approaches a constant value equal to the static depletion layer capacitance.

In the particular examples chosen, this occurs at frequencies $\gtrsim$200 Hz. The decrease in the effective dielectric constant with increasing frequency would appear to fit the empirical power-law relationship generally observed for biological materials (Fricke and Curtis, 1937).

The constancy of the capacitance at high frequencies, in relation to the conductance, and the rapid increase with decreasing frequency at low frequencies where the conductance is only slowly varying are illustrated in Fig. 5.

Phase Angle of the Dispersive Element

The phase angle of the frequency-dependent impedance as a function of frequency is shown in Fig. 6. It is evident that the phase angle, particularly for frequencies above 5 Hz, is a very slowly varying function of frequency, despite the fact that the parallel conductance and capacitance are very rapidly varying functions of frequency.

Effect of Asymmetrics in the Lattice Parameters

Apart from the opposite sign of their fixed charges, the two lattices of the double FCM may also have other asymmetries. These could include differences in the widths

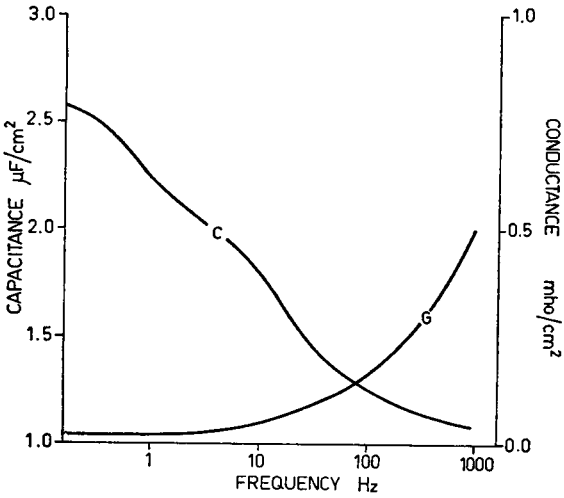

FIGURE 7

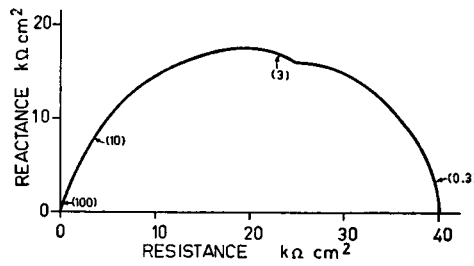

FIGURE 8

FIGURE 7 The parallel capacitance and conductance of a double FCM for which in one lattice $W^2/D = 0.1$ S and in the other $W^2/D = 2.5$ S. The total DC resistance of the membrane was kept at 40 kΩ cm².

FIGURE 8 A plot of the equivalent series reactance vs. the resistance of the system to which Fig. 7 refers.

of the N^+ and N^- lattices, differences in the concentrations of fixed charges and differences in the values for the diffusion constants of the coions in each lattice.

The presence of such asymmetries gives rise to more complicated dispersion curves. For small differences in $W_\pm^2/D$ only the total change in C and G and the frequency range over which these changes take place is affected.

When the values of $W_\pm^2/D$ for two or more ions are sufficiently different, separate phases in the dispersion curve can be distinguished. Such features show up in the double FCM, with the parameters used previously, when $W_\pm^2/D$ differ by more than a factor of 10. An example of such a dispersion curve is shown in Fig. 7 and the corresponding impedance locus is shown in Fig. 8.

DISCUSSION

It was seen (Fig. 5) that the magnitude of the dispersion is strongly dependent on the diffusion constants for the mobile ions. The dispersion described arises essentially from polarization effects in the diffusion of the mobile ions. While the characteristics of the double FCM are superimposed on the polarization effects, it is nevertheless not unexpected that the plots of the complex impedance are very similar to those given by Cole (see Fig. 2:57, Cole, 1968) for the diffusion polarization of a system of electrodes in a simple aqueous solution.

The theoretical results obtained are also in general agreement with the experimental results given by Schwartz and Case (1964) for the AC impedance of synthetic

fused anion-cation membranes in aqueous solutions of electrolytes. These workers anticipated that the observed behavior might be due to diffusion polarization effects. The complex impedance loci for these membranes (Fig. 6, Schwartz and Case, 1964) yielded segments of circular loci. This led them to analyze their results in terms of a Cole-type equivalent circuit for the membrane. In the light of the present work their results, which showed two distinct segments in the impedance loci, would indicate asymmetries in the lattice parameters such as those that gave rise to the features shown in Figs. 7 and 8. The variation of the phase angle with frequency obtained by Schwartz and Case for the synthetic membranes are also very similar to the theoretical curves shown in Fig. 6.

The general form of the theoretical dispersion curves are further very similar to those observed for the membranes of cells such as squid axons, muscle fibers, and lysed erythrocytes (e.g. see, Cole 1970; Falk and Fatt, 1964; Schwann, 1950, 1954, 1957). With the particular membrane parameters chosen, good quantitative agreement is obtained with the experimental results obtained with cells of *C. corallina*.[1] The more complicated features discussed earlier, when the various parameters for the two lattices and/or mobile ions are different, have also been observed in these experiments.

The relative constancy of the capacitance at high frequencies, where the conductance is increasing rapidly with frequency and the rapid increase in capacitance with decreasing frequency at very low frequencies, Fig. 5, is in line with the observations reported by Cole for starfish egg membranes (see Cole, 1970).

As pointed out earlier for cellular membranes, the diffusion constants in small discrete patches (e.g., "pores") may be considerably higher than in the rest of the membrane. As long as the ion profiles are established and *some* conduction takes place in the remainder of the membrane, however, the frequency-dependent diffusion capacitance will remain substantially as presented. The total conductance on the other hand is then dominated by the pore conductance which at low frequencies would be largely frequency independent. The conductance of the remainder of the membrane would contribute only a small but frequency-dependent component to the total conductance. It is also worth noting that the very high membrane capacitances measured at very low frequencies almost completely preclude the possibility that a major part of the membrane merely behaves as a static dielectric.

CONCLUSIONS

The analysis of the AC characteristics of the double fixed charge membrane model shows that:

(*a*) The parallel capacitance and conductance of the membrane undergo a strong dispersion at low frequencies.

(*b*) At very low frequencies the diffusion capacitance makes a large contribution to the total membrane capacitance.

(*c*) At high frequencies the membrane capacitance, which is then essentially frequency independent, is due to charge storage associated with modulation of the width of the depletion layer.

(*d*) The magnitude of the low frequency diffusion capacitance increases rapidly with decreasing values of the diffusion constants for the mobile ions in the membrane.

(*e*) The real vs. the imaginary parts of the complex impedance yield loci which are approximately semicircular.

(*f*) The theoretical dispersion characteristics are very similar to those observed for *C. corallina* at low frequencies and are compatible with those reported for other cellular membranes such as those of squid axons, muscle fibers, and red cell ghosts. The results are also in accord with those reported for a synthetic-fused anion-cation membrane.

APPENDIX

The general solution of Eq. 6 is:

$$P(x, t) = (C_1 \exp x \sqrt{K/D} + C_2 \exp - x \sqrt{K/D}) \exp Kt + h(x), \quad (A\,1)$$

where h is the DC component. The coion concentration at the depletion layer boundary at $x = -\lambda_+$ can also be obtained using the Boltzmann relation in Eq. 2 with the potential given by Eq. 7. This gives:

$$P_j(t) = p(x = -\lambda_+, t) = P_m \exp \frac{qV(\mathrm{DC})}{kT} \left[1 + \frac{q\tilde{V}}{kT} \exp j\omega t\right],$$

$$= P_j(\mathrm{DC}) + \tilde{P}_j \exp j\omega t, \quad (A\,2)$$

where

$$P_j(\mathrm{DC}) = P_m \exp \frac{qV(\mathrm{DC})}{kT},$$

and $\tilde{P}_j$, the amplitude of the AC variation in P_j is given by

$$\tilde{P}_j = P_j(\mathrm{DC}) \frac{q\tilde{V}}{kT} \exp j\omega t.$$

Comparison of the time-dependent terms in Eqs. A 1 and A 2 immediately yields $K = j\omega$ and hence,

$$P(x, t) = [C_1 \exp x \sqrt{j\omega/D} + C_2 \exp - x \sqrt{j\omega/D}] \exp j\omega t + h(x), \quad (A\,3)$$

where h is the DC component.

The constants C_1 and C_2 in this expression can be determined as follows: at the membrane boundary $x = -W$ the minority ion concentration is time independent [$P(x, t) = P_m$].

Thus with $x = -W$ Eq. A 3 yields

$$C_2 = -C_1 \exp\left(-2W\sqrt{\frac{j\omega}{D}}\right). \qquad (A\,4)$$

At the depletion layer boundary $x = -\lambda_+$ Eqs. A 3 and A 4 yield

$$P_j(t) = P(x = -\lambda_+, t)$$
$$= C_1\left[\exp\left(-\lambda_+\sqrt{\frac{j\omega}{D}}\right) - \exp\left((-2W + \lambda_+)\sqrt{\frac{j\omega}{D}}\right)\right].\exp j\omega t$$
$$+ P_j(\mathrm{DC}). \qquad (A\,5)$$

Comparison of Eq. A 5 with Eq. A 2 then gives

$$C_1 = \frac{\tilde{P}}{\left[\exp\left(-\lambda_+\sqrt{\frac{j\omega}{D}}\right) - \exp\left((-2W + \lambda_+)\sqrt{\frac{j\omega}{D}}\right)\right]},$$

or

$$C_1 = \frac{\tilde{P}_j \exp\left(+W\sqrt{\frac{j\omega}{D}}\right)}{\left[\exp\sqrt{\frac{j\omega}{D}\,W_+^2} - \exp -\sqrt{\frac{j\omega}{D}\,W_+^2}\right]}, \qquad (A\,6)$$

where $W_+ = W - \lambda_+$ is the width of the region in the positive-fixed charge lattice outside the depletion layer. With Eq. A 6, Eq. A 3 yields the expression 9 given in the text.

The author wishes to thank Professor E. P. George for his critical reading of the manuscript and his helpful suggestions.

He also wishes to thank the Australian Research Grants Committee for support for the conduct of this Research.

Received for publication 10 April 1972 and in revised form 17 July 1972.

REFERENCES

COLE, K. S. 1928. *J. Gen. Physiol.* **12**:37.
COLE, K. S. 1932. *J. Gen. Physiol.* **15**:641.
COLE, K. S. 1965. *Physiol. Rev.* **45**:340.
COLE, K. S. 1968. Membranes, Ions and Impulses. University California Press, Berkeley.
COLE, K. S. 1970. *In* Physical Principles of Biological Membranes. F. Snell, J. Wolken, G. J. Iverson, and J. Lam, editors. Gordon and Breach Science Publishers, Inc. New York.
COLE, K. S., and H. J. CURTIS. 1938. *J. Gen. Physiol.* **22**:37.
COLE, K. S., and H. J. CURTIS. 1939. *J. Gen. Physiol.* **22**:649.
COSTER, H. G. L. 1965. *Biophys. J.* **5**:669.
COSTER, H. G. L. 1969. *Aust. J. Biol. Sci.* **22**:365.
COSTER, H. G. L. 1972. *Biophys. J.* **12**:447.

COSTER, H. G. L. 1973. *Biophys. J.* **13**:133.
COSTER, H. G. L., E. P. GEORGE, and R. SIMONS. 1969. *Biophys. J.* **9**:666.
COSTER, H. G. L., and A. B. HOPE. 1968. *Aust. J. Biol. Sci.* **21**:243.
FALK, G., and P. FATT. 1964. *Proc. R. Soc. Lond. B Biol. Sci.* **160**:64.
FRICKE, H., and H. J. CURTIS. 1937. *J. Phys. Chem.* **41**:729.
MAURO, A. 1962. *Biophys. J.* **2**:179.
OFFNER, F. F. 1969. *Bull. Math. Biophys.* **31**:359.
SCHWANN, H. P. 1950. *Am. J. Physiol.* **163**:748.
SCHWANN, H. P. 1954. *Z. Naturforsch. Teil. B.* **9**:245.
SCHWANN, H. P. 1957. *Adv. Biol. Med. Phys.* **5**:147.
SCHWANN, H. P., and E. CARSTENSEN. 1957. *Science (Wash. D. C.).* **125**:985.
SCHWARTZ, M., and C. T. CASE. 1964. *Biophys. J.* **4**:137.